Applied Acoustics 216 (2024) 109788

Contents lists available at ScienceDirect

Applied Acoustics

journal homepage: www.elsevier.com/locate/apacoust

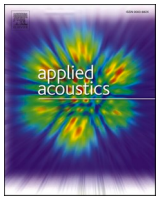

Technical note

Fabrication of Micro-Perforated Panel (MPP) sound absorbers using Digital Light Processing (DLP) 3D printing technology

J. Carbajo [a,*], S.-H. Nam [b], N.X. Fang [b,c]

[a] University of Alicante, Department of Physics, Systems Engineering and Signal Theory, San Vicente del Raspeig, Spain
[b] Massachusetts Institute of Technology, Department of Mechanical Engineering, Cambridge, MA 02139, USA
[c] University of Hong Kong, Department of Mechanical Engineering, Pokfulam Road, Hong Kong 999077, PR China

ARTICLE INFO

Keywords:
Sound absorption
Micro-Perforated Panel (MPP)
Additive manufacturing (AM)
Digital Light Processing (DLP) technology

ABSTRACT

The fabrication of Micro-Perforated Panels (MPPs) still constitutes a challenge to the acoustic materials industry because it usually requires expensive manufacturing techniques to obtain holes of submillimetre size. In this context, the rise of additive manufacturing or 3D printing (3DP) technologies over the last years has paved the way for the design and development of new materials at the microscopic scale. Among these, Digital Light Processing (DLP) technology emerges as an excellent option due to its advantages in terms of printing speed and higher accuracy when compared to traditional additive manufacturing technologies. This work demonstrates the capacity of DLP technology to fabricate MPPs and explores its design possibilities by using different exposure times in the manufacturing process to attain different hole sizes. To this end, several MPP specimens were fabricated and tested when used as a resonator system in an impedance tube setup to determine their sound absorption performance, the experimental data showing a good agreement when compared to predictions obtained using the Maa model. Preliminary results highlight the potential capabilities of DLP and encourage its use in the design stage of these acoustics resonator systems.

1. Introduction

Micro-Perforated Panel (MPP) sound absorbers have been extensively used in many noise reduction applications since their early introduction by Maa [1]. When used as acoustic resonators, these devices achieve useful sound absorption performance in room acoustics [2], outdoor noise barriers [3], and muffler devices [4]. Perforated panels are usually manufactured from metal, wood, or plastic; being one of the main challenges in their fabrication accurately achieving small holes. Some of the most extended fabrication techniques for the development of MPPs range from the use of mechanical drilling or milling bits to waterjet machines and laser cutting systems. Unfortunately, the former approaches may severely damage the panel and change the materials surrounding the drilled hole, thus influencing the resulting acoustic performance of the sound absorber, whereas the latter are commonly considered too expensive for many applications. Alternatively, some authors have proposed fabrication techniques based on the infiltration process [5], mold manufacturing and casting technologies [6], and heat shrinkage [7]. In this context, Additive Manufacturing (AM) techniques constitute an excellent alternative workbench because of the engineering capabilities for the development of innovative designs that yield outstanding sound absorption properties [8].

These also called 3DP (3D printing) technologies have not only revolutionized some industrial fabrication sectors but also led to a relevant paradigm shift both in economic and productive terms. In this context, the development of acoustic materials using AM technologies has shown the extraordinary capabilities and potential use thereof in many applications of acoustics engineering [9]. Several examples of the use of these technologies in the fabrication of MPPs can be found in the literature. Liu et al. [10] investigated the absorption capabilities of multi-layer micro-perforated panel absorbers whose front layer was produced using additive manufacturing stereolithography (SLA) technology. Akiwate et al. [11] analysed the acoustic properties of additively manufactured MPPs with different perforation shapes (circular, triangular, and square) backed by a periodic honeycomb structure by using Fused-Deposition Modeling (FDM) technology. Carbajo et al. [12] studied the acoustic behaviour of perforated panel absorbers with straight and oblique perforations fabricated using Projection micro-stereolithography (PμSL).

One of the main challenges when using these technologies is the

* Corresponding author.
E-mail addresses: jesus.carbajo@ua.es (J. Carbajo), shnam@mit.edu (S.-H. Nam), nicfang@mit.edu, nicxfang@hku.hk (N.X. Fang).

https://doi.org/10.1016/j.apacoust.2023.109788
Received 6 September 2023; Received in revised form 27 November 2023; Accepted 28 November 2023
Available online 1 December 2023

verification of the design models from the fabricated materials due to the printing accuracy, especially in the case of narrow geometries. Zieliński et al. [13] found that the acoustical properties of porous samples 3D-printed using Fused Deposition Modelling (FDM) technology differ from those predicted using well-established theoretical models. The authors concluded that these discrepancies may not only be attributed to accuracy causes but also to imperfections resulting from micro-fibers, micro-pores, and pore surface roughness. In the case of MPPs, these accuracies are mainly attributed to the shape and profile of the printed perforations across the panel. Sakagami et al. [14] analysed the effect of deviation due to the manufacturing accuracy on the trial production of MPPs of different hole shapes. In their work, large deviations were observed between theoretical sound absorption results and experimental tests over MPPs printed using a consumer-grade additive manufacturing 3D printer that uses FDM technology.

An exhaustive inter-laboratory test on the suitability of different additive manufacturing technologies to reproduce porous samples designed for sound absorption can be found in [15]. In that work, it was noted the absorption curves for samples manufactured using DLP avoided imperfections attributed to filament deposition (e. g. small fibers inside voids) also yielding smoother surfaces. Given the higher printing speed, better surface finish, and improved accuracy of DLP over FDM, it turns out of great interest to further explore its printing possibilities, especially for rapid prototyping of acoustic materials.

This technical note is aimed at exploring the possibilities of DLP technology for the fabrication of MPPs when used as acoustic resonators. Several specimens were prepared using DLP technology and tested in an impedance tube following the procedure described in the ISO 10534-2 standard [16] to assess their sound absorption performance. Experimental results showed a good agreement when compared to predictions obtained using the theoretical model for MPPs proposed by Maa for a design case Besides, it was shown that by overcuring the samples during the fabrication process, smaller perforations with a tapered profile (i.e. perforations with a varying cross-section) can be achieved, its influence on the sound absorption performance of the acoustic resonator being also discussed. This preliminary work shows the higher accuracy and potential capabilities of DLP technology in the fabrication of MPPs, thus encouraging its use in the design stage of resonant sound absorbers.

This technical note is organized as follows: in Section 2, the background theory necessary to understand the acoustic behaviour of MPP sound absorbers and the well-known Maa analytical model used to predict it are presented. Section 3 highlights the main advantages of using DLP technology when compared to other 3DP technologies and describes the fabrication procedure followed to prepare the MPP specimens with different exposure times (i.e. overcuring time). In Section 4, results on the geometrical and acoustical characterization of the fabricated samples are given, along with a comparison of the measured sound absorption data with the Maa model predictions and some remarks on the use of DLP to study MPPs. Finally, the main conclusions of this work are summarized in Section 5.

2. Background theory

2.1. MPP sound absorbers

Micro-Perforated Panels (MPPs) consist of a flat rigid surface whose perforations (typically circular holes or slits) are distributed periodically, the sound attenuation being produced by viscous friction and thermal conduction in the inner air of the perforations. Unlike ordinary perforated panels, the higher acoustic resistance due to the submillimetric size of the holes results in an increased absorption bandwidth when used as a resonator system. These resonator systems can be achieved by spacing the MPP from a rigid wall by an air cavity, its sound absorption performance is determined by the size of the perforations, the open area ratio (or perforation rate), the panel thickness, and the depth of the air cavity. Several models for the modeling of MPPs exist in the literature [17,18], the one proposed by Maa being one of the most extended because of its simplicity and ease of use as it will be described next.

2.2. Maa model for MPP sound absorbers

Let us consider an MPP of thickness t with circular cross-section perforations of diameter d backed by an air cavity of depth L as depicted in Fig. 1.

According to Maa [17], the acoustic transfer impedance Z of the MPP under normal incidence can be obtained from

$$Z = \frac{1}{\phi}\left(\frac{32\eta t}{d^2}\left(\sqrt{1+\frac{x^2}{32}}+\frac{\sqrt{2}}{32}x\frac{d}{t}\right)+j\omega\rho_0 t\left(1+\frac{1}{\sqrt{1+\frac{x^2}{2}}}+0.85\frac{d}{t}\right)\right) \tag{1}$$

where $\phi = \pi(d/2)^2/b^2$ is the open area ratio of the panel, being b the distance between perforations, η is the dynamic viscosity of air, and $x = d(\omega\rho_0/(4\eta))^{1/2}$, where ω is the angular frequency and ρ_0 the air density.

The surface impedance Z_S of the whole resonator system is then given by

$$Z_S = Z - jZ_0\cot\left(\frac{\omega}{c_0}L\right) \tag{2}$$

where $Z_0 = \rho_0 c_0$ is the characteristic impedance in air, c_0 being the speed of sound in air.

Thereby, the sound absorption coefficient α can be calculated as [19]

$$\alpha = 1 - \left|\frac{Z_S - Z_0}{Z_S + Z_0}\right|^2 \tag{2}$$

3. Additive manufacturing using DLP

3.1. DLP technology

Fused Filament Deposition (FFD) and stereolithography (SLA) are the two most used additive manufacturing technologies in the field of acoustic materials because of the ease of quickly producing a 3D channel net network with high aspect ratio features at a low cost. However, these technologies exhibit a significant drawback in terms of accuracy as it is difficult to secure a sophisticated channel of less than 500 μm due to the curing process involved in the sequential addition of patterned layers [20]. Using DLP allows controlling the size of the channel through which air passes by applying the horizontal direction overcuring reaction. In doing so, the diameter of the channels can be systematically controlled with a sub-pixel size, thus minimizing the overcuring effect and increasing the printing accuracy. Besides, given that each printed layer is cured at once it is much faster than conventional SLA technology. All these features make DLP a good candidate for the additive manufacturing of MPPs whose fabrication procedure will be described next.

3.2. Fabrication of MPPs using DLP technology

To study the influence of the curing process on the "effective" final size of the MPP perforations, several samples were prepared using an exposure time that ranged in the interval from 10 s to 26 s. Fig. 2a shows a schematic representation of the fabrication of MPP samples using DLP 3D printing (3DP) technology. OpenSCAD was used to design the 3D geometric model of each MPP, which consisted of circular samples 30 mm in diameter and a thickness $t = 0.05$ mm with periodically distributed circular holes of diameter $d = 0.16$ mm spaced $b = 1.9$ mm. It should be mentioned that the choice of these initial geometrical characteristics was made after some preliminary tests using the previously

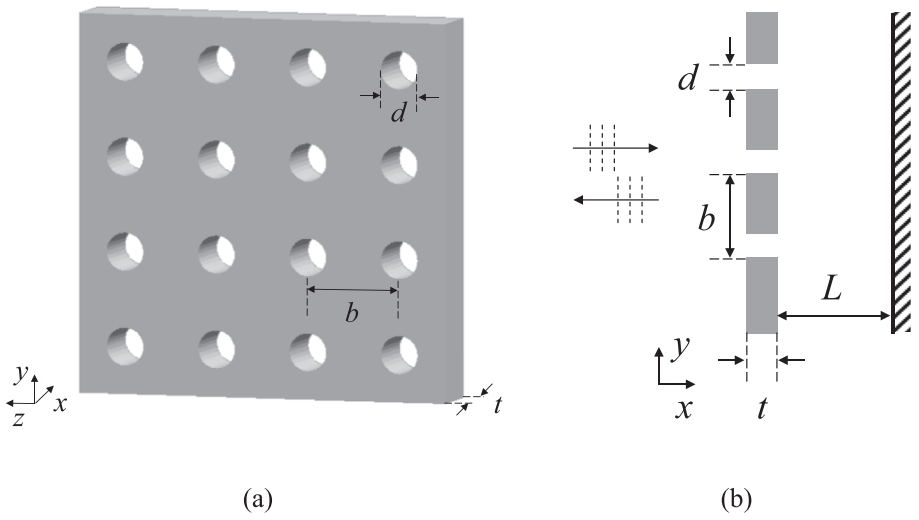

Fig. 1. Schematic representation of a MPP: (a) Detailed view; and (b) backed by an air cavity to achieve an acoustic resonator.

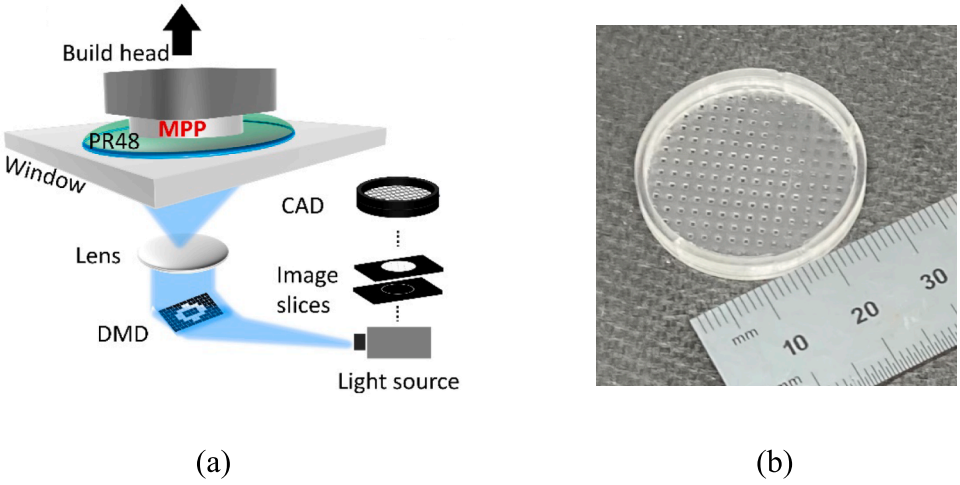

Fig. 2. (a) Fabrication of the MPP samples using DLP 3D printing (3DP) technology, (b) detailed view of a printed MPP obtained from the MPP design image.

described Maa model to achieve maximum sound absorption amplitude at resonance and served to illustrate the effect of DLP exposure time on the absorption performance, as it will be shown in the results. CAD files were exported in STL format and then imported into Autodesk's Print Studio software to generate 2D slice images with a thickness of 50 μm and exported as.tar.gz files without adding supports around the build area. The files were uploaded to the Autodesk Ember (XY resolution of 50 μm and Z resolution from 10 to 100 μm) and printed using Clear type PR48 resin, the patterning in the photopolymer resin being transferred by projecting the binary layer image using DLP. In brief, the build head was lowered into a resin vat a distance of 50 μm from the printing window, whereby a 2D digital image was projected to crosslink the resin in regions exposed to light. The process was repeated layer-by-layer until each full 3D structure was obtained. Each MPP was monolithically integrated with external rings at the top and bottom to enhance mechanical stability and ensure good panel sealing in the subsequent impedance tube testing. Printed MPPs were removed from the build head, soaked in isopropanol for 10 min to remove monomer from the unexposed regions, and then dried resulting in samples as that shown in Fig. 2b.

4. Results and discussion

4.1. Geometrical characterization of the fabricated MPP samples

First, a geometrical characterization of the fabricated samples was performed using an optical microscope. Fig. 3a shows microscopic images of the holes obtained for four of the fabricated MPP samples whose exposure times were 10 s, 18 s, 20 s, and 23 s. These images indicate that as the exposure time increases, the transversal profile of the perforation gets tapered in the central region resulting in a hole with a varying cross-section and whose "effective" size diminishes. Hence, the attenuation produced in these perforations and consequently the sound absorption performance of these MPPs when used as acoustic resonators is expected to depend on the exposure time. A more detailed analysis of this effect is shown in Fig. 3b, which plots the average perforation diameter (black square markers) and overcured part size (blue square markers) as a function of the exposure time, the red circular markers standing for the sum of both sizes. It can be seen a slow decrease in the hole size from 10 to 17 s and a rapid decrease when the exposure time exceeds 18 s, 20 s being the photo-curing time required to form pores of the designed size. When the exposure time exceeds 23 s the truncation disappears and the cured resin in the pixel-off area fills all the pores.

The above-mentioned tapering effect can be attributed to the indirect

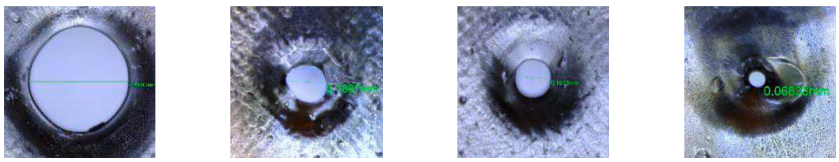

Exp. time: 10 sec (d = 0.460 mm) | Exp. time: 18 sec (d = 0.189 mm) | Exp. time: 20 sec (d = 0.163 mm) | Exp. time: 23 sec (d = 0.068 mm)

(a)

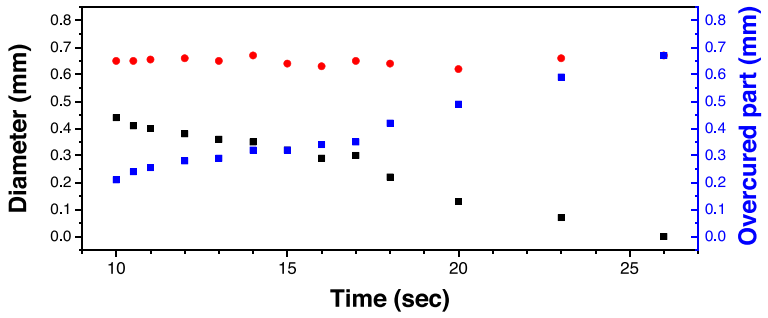

(b)

Fig. 3. Geometrical characterization of the MPP samples fabricated using DLP technology: (a) Microscopic images of MPP samples fabricated with different exposure times (corresponding hole diameters d in parenthesis): 10 s, 18 s, 20 s, and 23 s, and (b) hole diameter (black square markers) and overcured part size (blue square markers) as a function of the exposure time (red circular markers stand for the sum of both sizes).

crosslinking by waveguide mode, which makes a stair-like truncation shape appear on each layer in the 3D printed microstructure made with DLP technology. Sun et al. [21] explained that diffraction and aberration of light induce truncations into parts produced by micro-stereolithography. The light per unit area is greater for large parts where light from neighboring pixels adds together resulting in the formation of truncation in the resin of the pixel-off area as additional and indirect photocuring. This generated truncation was applied to control the "effective" diameter of the pores of the MPP samples (i.e. the pixel-off area was used to indirectly control through the light exposure of the pixel-on area). As a result, indirect photo-crosslinking made it possible to obtain sub-pixel size pores that could not be fabricated with on–off control of DMDs (Digital Micromirror Devices). Regarding the exposure time necessary to obtain some designated design parameters, it is expected to depend on the size of the holes and thickness of the panel to be fabricated.

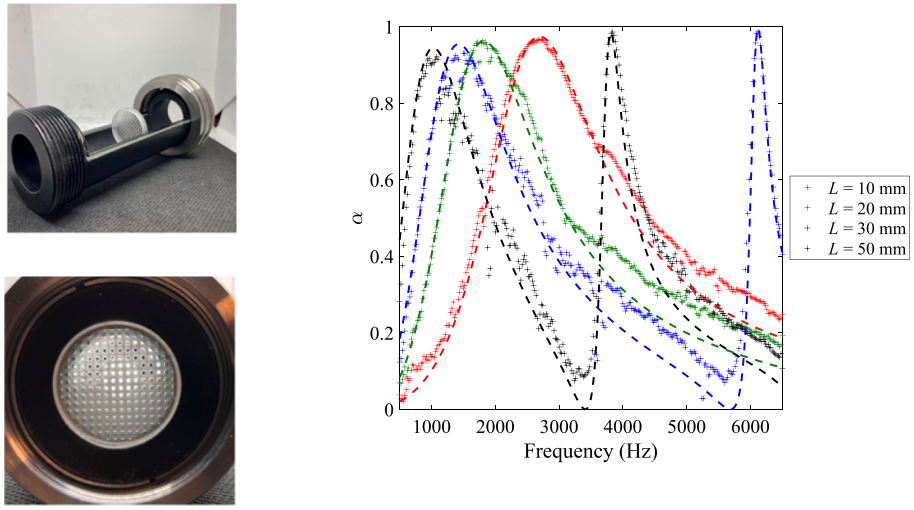

(a) (b)

Fig. 4. (a) Pictures of the acoustic characterization of the MPP printed samples following the procedure described in the ISO 10534-2: (Top) Sample holder, (Bottom) frontal view of the mounting on the impedance tube, and (b) comparison of the measured (cross markers) and predicted (discontinuous lines) sound absorption coefficient α for different air cavity depth L values (10 mm, 20 mm, 30 mm, and 50 mm).

4.2. Acoustical characterization of the fabricated MPP samples

Once the geometrical characterization of the fabricated samples was finished, impedance tube experiments were performed by following the transfer function method procedure described in the ISO10534-2 standard [16]. This method was used both to assess the sound absorption performance of the prepared specimens and to verify the fabrication accuracy of the DLP technology by comparing the absorption results with the theoretical predictions of the Maa model for the designed MPP. For this purpose, SW470 impedance tube equipment was used together with VAL-Lab2 software, and the sound absorption coefficient under normal incidence of the fabricated samples was measured. Fig. 4a shows a general view of the impedance tube setup and a detailed view of the sample holder used in the experiments. Several acoustic resonator configurations were tested for the reference MPP design (exposure time of 20 s). Specifically, air cavity depths in the range from 10 mm to 50 mm were tested. Fig. 4b shows a comparison of the measured and predicted sound absorption coefficient for different air cavity depth configurations.

Sound absorption results show that the predictions agree well with the measured data for the design case. In general, all the resonator configurations show a good sound absorption performance both in terms of maximum sound absorption (peak values above 0.9) and absorption bandwidth (up to 2700 Hz). It should be noted that those perforations at the perimeter of the sample (i.e., closer to the impedance tube walls) have different boundary conditions than those in the inner region, thus yielding some deviations when comparing the experiments to the theoretical predictions. Moreover, the resulting tapered profile is also expected to slightly influence the dissipation phenomena through the holes, a brief discussion on this effect being given in the remarks of Section 4.3.

Additionally, impedance tube tests were performed over the remaining fabricated MPP samples to analyse the effect of exposure time of DLP technology on their sound absorption performance. Fig. 5 shows the measured sound absorption data for MPP samples whose exposure times were 10 s, 18 s, 20 s, and 23 s when used as an acoustic resonator with air cavity depth $L = 10$ mm.

Results indicate that as the exposure time increases, the sound absorption peak shifts to lower frequencies from 5000 Hz (exposure time 10 s) down to 2600 Hz for the design case (exposure time 20 s) and 1100 Hz for the smallest hole size (exposure time 23 s) while still showing a good sound absorption performance for most cases (amplitude values above 0.8 at resonance). This tuning capability may be of great interest in the fabrication of MPPs with different geometrical characteristics and highlights the potential design capabilities of DLP technology.

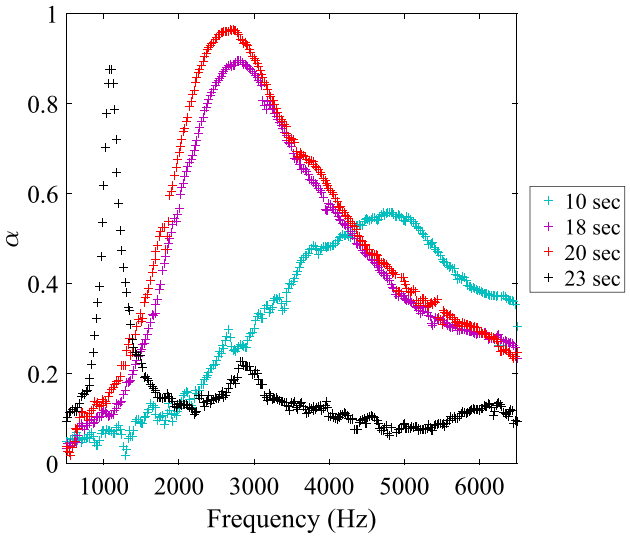

Fig. 5. Measured sound absorption coefficient α of the MPP samples fabricated using DLP technology with different exposure times: 10 s, 18 s, 20 s, and 23 s (acoustic resonator with air cavity depth $L = 10$ mm).

4.3. Remarks on the use of DLP technology to fabricate MPPs

Previous results not only show that an MPP design can be accurately fabricated using DLP technology but also that excellent sound absorption can be achieved when used as acoustic resonators. However, some remarks must be drawn from the microscopic images and impedance tube experiments.

First, as the exposure time increases, a directly cured part (panel) and an indirectly cured part (perforation) are obtained, as it was shown in the microscopic images of Fig. 3a. This is a result of the overcuring mechanism schematically depicted in Fig. 6, which shows that direct photocuring by projected beam forms the MPP until it gets fully cured but indirect photocuring occurs by a waveguide effect as the exposure time keeps rising until the perforations are closed. Some approaches to minimize overcuring are doping light absorber in the monomer resin [22], improving the system hardware and optical components to adjust the light dosage and curing depth [23–25], or designing the structure to avoid light leaks [26]. The listed approaches prevent the curing of the remaining monomers within the cured and 3D-printed channel network by chemically or physically inhibiting light from penetrating deeper than the specified layer thickness. Unfortunately, despite successfully controlling light transmission in the vertical direction, overcuring in the horizontal direction still exists [23–25], the convex shape observed in all stacked layers being proof of that (i. e. an area that is not directly exposed to light, but is indirectly exposed to light due to scattering and refraction). Additional crosslinking inevitably occurs, resulting in an arcuate profile in the vertical direction of the layers of the printed samples. Consequently, these changes in light exposure and intensity indirectly show significant differences in the size and shape of the overcured area [21,27,28].

In summary, the fabrication of micro-perforated panels using DLP technology yields tapered perforation whose final hole size depends on the overcuring time. One of the main advantages of this overcuring process is that hole sizes smaller than the printer resolution can be achieved, thus overcoming 3DP accuracy limitations linked to the DMD chip. This feature may ease the fabrication of sub-millimetric perforations to broaden the sound absorption bandwidth up to 3 or 4 octaves and hence improve the acoustic resonator performance, especially in the low-frequency range [17]. As for the tapered hole profile, several authors have shown that these hole shapes may improve the sound absorption performance of MPP sound absorbers [29], especially in the case of thick MPPs [30], the use of numerical prediction approaches based on CFD [31] or finite elements [32] being very useful for the better understanding of the underlying acoustic phenomena. In this regard, the modeling and analysis of the tapered hole shapes obtained when using additive manufacturing technologies constitutes an issue that needs further research in the forthcoming years [33]. Besides, modifications of the Maa model would be necessary to account for the induced vibration of the MPP or the hole interaction effect, especially in the case of thin panels or panels with closely spaced holes, respectively. These extra phenomena may affect the absorber performance and therefore should be considered in the design stage using the Fok function [34] or an acoustic-structural analysis [35].

5. Conclusions

This technical note was focused on the fabrication of MPPs using DLP technology. Unlike more widespread technologies such as FFD, DLP technology shows a smaller feature size at a faster delivery rate and overcomes several drawbacks of the former (e.g. imperfections resulting from micro-fibers, micro-pores, and pore surface roughness). Also, it is a cost-effective technique in terms of productivity due to the low material

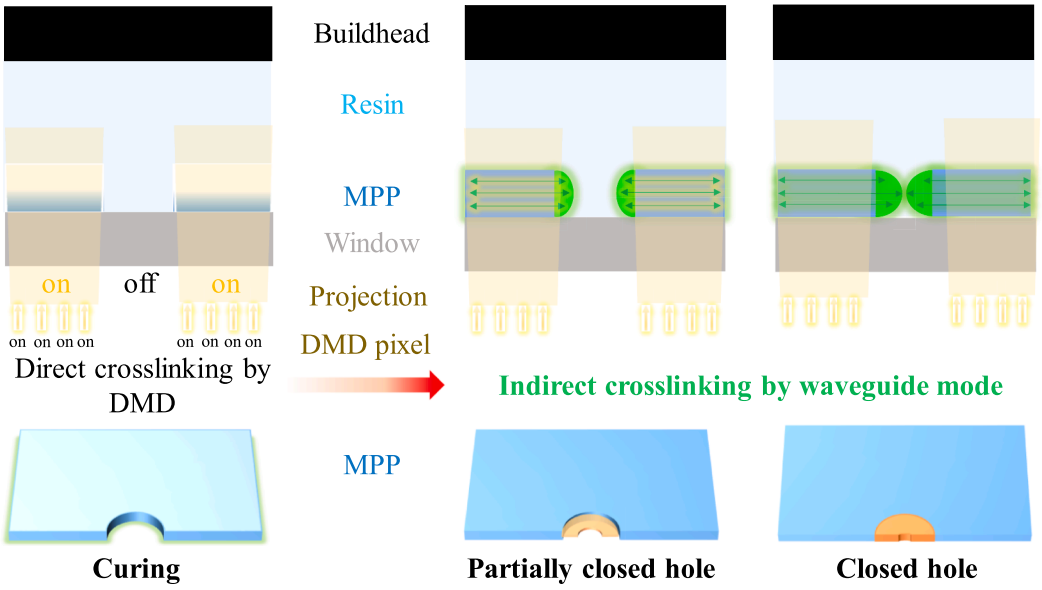

Fig. 6. Schematic representation of the overcuring mechanism in the fabrication of MPPs using DLP technology.

consumption and small footprint, thus encouraging its use to increase the accuracy in the fabrication of 3D-printed materials as is the case of MPPs. Several specimens were manufactured and tested using the standardized procedure described in the ISO10534-2 to obtain their sound absorption coefficient when used as acoustic resonator systems. It was found that this technology not only allows the fabrication of these acoustic materials with high printing accuracy (as confirmed by predictions using the well-known Maa model for MPP sound absorbers) but also the reduction of the perforation size as the exposure time increases, being that one of the greatest challenges in the fabrication of perforated panels with sub-millimetric holes. This overcuring effect not only reduced the hole size but also shifted the sound absorption resonance peak of these MPPs to lower frequencies as demonstrated by experiments over the fabricated samples. On the other hand, microscopic images showed that the 3D printing process yields a directly cured region and an indirectly cured region which results in a tapering effect that may improve the sound attenuation in the MPPs. In conclusion, preliminary results show the design capabilities of DLP technology to successfully fabricate MPPs, further research being encouraged to study the interesting tapering effect and its harness in the design stage thereof.

CRediT authorship contribution statement

J. Carbajo: Conceptualization, Investigation, Methodology, Writing – original draft. **S.-H. Nam:** . **N.X. Fang:** .

Declaration of competing interest

The authors declare that they have no known competing financial interests or personal relationships that could have appeared to influence the work reported in this paper.

Data availability

Data will be made available on request.

Acknowledgments

The conception of this research work took place at the Department of Mechanical Engineering at the Massachusetts Institute of Technology with support from the University of Alicante (Grant ACIE20-04).

References

[1] Maa DY. Theory and design of microperforated sound-absorbing constructions. Sci Sin 1975;18(1):55–71.
[2] Fuchs HV, Zha X. Acrylic-glass sound absorbers in the plenum of the Deutscher Bundestag. Appl Acoust 1997;51(2):211–7.
[3] Adrubali F, Pispola G. Properties of transparent sound-absorbing panels for use in noise barriers. J Acoust Soc Am 2007;121(1):214–21.
[4] Munjal ML. Acoustic of ducts and mufflers. Chichester (United Kingdom): John Wiley and Sons; 2014.
[5] Cobo P, Montero F. Proposal of cheap microperforated panel absorbers manufactured by infiltration. Appl Acoust 2013;74:1069–75.
[6] Qian YJ, Kong DY, Fei JT. A note on the fabrication methods of flexible ultra micro-perforated panels. Appl Acoust 2015;90:138–42.
[7] Gai X-L, Xing T, Cai Z-N, Wang F, Li X-H, Zhang B, et al. Developing a microperforated panel with ultra-micro holes by heat shrinkable materials. Appl Acoust 2019;152:47–53.
[8] Setaki F, Tenpierik M, Turrin M, van Timmeren A. Acoustic absorbers by additive manufacturing. Build Environ 2014;72:188–200.
[9] Suárez L, Espinosa MM. Assessment on the use of additive manufacturing technologies for acoustic applications. Int J Adv Manuf Technol 2020;109:2691–705.
[10] Liu Z, Zhan J, Fard M, Davy JL. Acoustic properties of multilayer sound absorbers with a 3D printed micro-perforated panel. Appl Acoust 2017;121:25–32.
[11] Akiwate DC, Date MD, Venkatesham B, Suryakumar S. Acoustic characterization of additive manufactured perforated panel backed by honeycomb structure with circular and non-circular perforations. Appl Acoust 2019;155:271–9.
[12] Carbajo J, Ghaffari Mosanenzadeh S, Kim S, Fang NX. Sound absorption of acoustic resonators with oblique perforations. Appl Phys Lett 2020;116:054101.
[13] Zieliński TG, Dauchez N, Boutin T, Leturia M, Wilkinson A, Chevillotte F, et al. Taking advantage of a 3D printing imperfection in the development of sound absorbing materials. Appl Acoust 2022;197:108941.
[14] Sakagami K, Kusaka M, Okuzono T, Nakanishi S. The effect of deviation due to the manufacturing accuracy in the parameters on an MPP on its acoustic properties: trial production of MPPs of different hole shapes using 3D printing. Acoustics 2020;2(3):605–16.
[15] Zieliński T, Opiela KC, Pawłowski P, Dauchez N, Boutin T, Kennedy J, et al. Reproducibility of sound-absorbing periodic porous materials additive manufacturing technologies: Round robin study. Addit Manuf 2020;36:101564.
[16] ISO 10534-2. Determination of sound absorption coefficient and impedance in impedance tubes (international organization for standardization), Switzerland; 1998.
[17] Maa DY. Potential of microperforated panel absorber. J Acoust Soc Am 1998;104(5):2861–6.
[18] Atalla N, Sgard JF. Modeling of perforated plates and screens using rigid frame porous models. J Sound Vib 2007;303:195–208.
[19] Allard JF, Atalla N. Propagation of sound in porous media. Modelling sound absorbing materials. Chichester (United Kingdom): John Wiley and Sons; 2009.
[20] Chen PC, Chen PT, Vo TNA. Using stereolithographic printing to manufacture monolithic microfluidic devices with an extremely high aspect ratio. Polym J 2021;13:3750.
[21] Sun C, Fang N, Wu DM, Zhang X. Projection micro-stereolithography using digital micro-mirror dynamic mask. Sens Actuators Phys 2005;121:113–20.

[22] Kowsari K, Zhanga B, Panjwani S, Chen Z, Hingorani H, Akbari S, et al. Photopolymer formulation to minimize feature size, surface roughness, and stair-stepping in digital light processing-based three-dimensional printing. Addit Manuf 2018;24:627–38.
[23] Gong H, Beauchamp M, Perry S, Woolley AT, Nordin G. Optical approach to resin formulation for 3D printed microfluidics. RSC Adv 2015;5:106621–32.
[24] Janusziewicz R, Tumbleston JR, Quintanilla AL, Mecham SJ, DeSimone JM. Layerless fabrication with continuous liquid interface production. Proc Natl Acad Sci 2016;113(42):11703–8.
[25] Tumbleston JR, Shirvanyants D, Ermoshkin N, Janusziewicz R, Johnson AR, Kelly D, et al. Continuous liquid interface production of 3D objects. Science 2015; 347(6228):1349–52.
[26] O'Neill PF, Kent N, Brabazon D. Mitigation and control of the overcuring effect in mask projection micro-stereolithography. AIP Conf Proc 2017;1896:200012.
[27] Vallejo-Melagarejo LD, Reifenberger RG, Newell BA, Narvaez-Tovar CA, Garcia-Bravo JM. Characterization of 3D-printed lenses and diffraction gratings made by DLP additive manufacturing. Rapid Prototyp J 2019;25(10):1684–94.
[28] Johnson AB, Procopio AT. Low cost additive manufacturing of microneedle maters. 3D Prin Med 2019;5(2).
[29] Randeberg RT. Perforated panel absorbers with viscous energy dissipation enhanced by orifice design. PhD Thesis, Trondheim, Norway; 2000.
[30] Sakagami K. A pilot study on improving the absorptivity of a thick micropeforated panel absorber. Appl Acoust 2008;69:179–82.
[31] Herdtle T, Bolton JS, Kim NN, Alexander JH, Gerdes RW. Transfer impedance of microperforated materials with tapered holes. J Acoust Soc Am 2013;134(6): 4752–62.
[32] Temiz MA, López I, Efraimsson G, Åbom M, Hirschberg A. The influence of edge geometry on end-correction coefficients in micro perforated plates. J Acoust Soc Am 2015;138(6):3668–77.
[33] Jafar NA, Ooi LE, Ripin ZM, Hi K, Yahaya AF. Resistance end correction of microperforated panel made using additive manufacturing. Eng Sci Technol Int J 2021;24:1281–91.
[34] Tayong R, Dupont T, Leclaire P. Experimental investigation of holes interaction effect on the sound absorption coefficient of micro-perforated panels under high and medium sound levels. Appl Acoust 2011;72:777–84.
[35] Bravo T, Maury C, Pinhède C. Vibroacoustic properties of thin micro-perforated panel absorbers. J Acoust Soc Am 2012;132:789–98.